ation for FISH as 60% (0.75 × 0.95 × 0.85). The validity of this estimation was demonstrated when the same calculation was applied to GFP experiments. The maximum detection of acentric minichromatid dissociation was estimated as 39%, a value very similar to the actual measured value.
11. P. Megee and D. Koshland, unpublished observation.
12. J. H. Hegemann and U. N. Fleig, *Bioessays* **15**, 451 (1993).
13. A. A. Hyman and P. K. Sorger, *Annu. Rev. Cell Dev. Biol.* **11**, 471 (1995).
14. M. Saunders, M. Fitzgerald-Hayes, K. Bloom, *Proc. Natl. Acad. Sci. U.S.A.* **85**, 175 (1988).
15. P. B. Meluh and D. Koshland, *Genes Dev.* **11**, 3401 (1997).
16. P. K. Sorger *et al.*, *Proc. Natl. Acad. Sci. U.S.A.* **92**, 12026 (1995).
17. Supported in part by NIH grant GM41718. We thank M. K. Raghuraman and R. Ciosk for plasmids and C.-M. Fan, V. Guacci, P. Meluh, and members of the Koshland Laboratory for valuable comments on the manuscript. P.C.M. was the recipient of a Cancer Research Fund of the Damon Runyon–Walter Winchell Foundation Fellowship DRG-1335.

1 April 1999; accepted 1 June 1999

Reach Plans in Eye-Centered Coordinates

Aaron P. Batista,* Christopher A. Buneo, Lawrence H. Snyder,† Richard A. Andersen‡

The neural events associated with visually guided reaching begin with an image on the retina and end with impulses to the muscles. In between, a reaching plan is formed. This plan could be in the coordinates of the arm, specifying the direction and amplitude of the movement, or it could be in the coordinates of the eye because visual information is initially gathered in this reference frame. In a reach-planning area of the posterior parietal cortex, neural activity was found to be more consistent with an eye-centered than an arm-centered coding of reach targets. Coding of arm movements in an eye-centered reference frame is advantageous because obstacles that affect planning as well as errors in reaching are registered in this reference frame. Also, eye movements are planned in eye coordinates, and the use of similar coordinates for reaching may facilitate hand-eye coordination.

To reach toward an object, information about its location must first be obtained from the retinal image. Early visual cortical areas contain topographic maps of the retina, and as a result the target is originally represented in eye-centered coordinates. However, targets for reaches should ultimately be represented in limb coordinates that specify the direction and amplitude the limb must move (motor error vector) to obtain its goal. Thus, for the brain to specify an appropriate reach command, coordinate transformations must take place. Transformation of signals from eye to limb coordinates requires information about eye, head, and limb position. These signals could be combined all at once to accomplish this transformation or in serial order to form intermediate representations in head-centered coordinates (by adding eye position information) and body-centered coordinates (by adding eye and head position information) (*1*). At some point in this process a plan to make the movement is formed; knowing how reach plans are represented in the brain can tell us much about the mechanisms and strategies the brain uses to generate reaches.

The major anatomical pathway for visually guided reaching begins in the visual cortex and passes through the posterior parietal cortex (PPC) to the frontal lobe. Different regions of PPC have recently been shown to be specialized for planning different types of movements (*2, 3*), including areas specialized for saccadic eye movements [the lateral intraparietal area (LIP)], for reaches [the parietal reach region (PRR)], and for grasping (the anterior intraparietal area). In other words, at this level of the visual-motor pathway the pattern of neural activity reflects the outcome of a movement selection process. Because PPC is partitioned into planning regions for different actions, it has been proposed that each subdivision should code its respective movement in the coordinate frame appropriate for making the movement (*4*). This proposal predicts that targets for reaches should be coded in limb coordinates in PRR. Here we demonstrate that the responses of reach-specific neurons in PRR are more consistent when reach targets are described in eye coordinates than in arm coordinates, showing that, at least in PRR, early reach plans are coded in terms of visual space rather than in terms of the limb.

Single cell recordings were made in PRR (*5*). We tested neurons in four conditions; in two conditions different reaches were performed to targets at the same retinal location, and in the other two conditions identical reaches were made to targets at different retinal locations (*6*). This paradigm allowed us to observe independently the effects on PRR neurons of manipulating target location in eye and limb reference frames. A reach-specific neuron tested in these four conditions is shown in Fig. 1. The effect of varying the initial hand position is shown in Fig. 1, A and B; the cell's spatial tuning is similar in the two conditions, showing that the cell is largely insensitive to changes in the limb-centered positions of the targets. The effect of changing the direction of gaze is shown in Fig. 1, C and D. The cell's spatial tuning changes markedly between these two conditions, even though the arm-centered locations of the targets do not change. In all conditions, the cell's preferred reach end point is constant relative to the direction of gaze—down with respect to fixation. This neuron is selectively active for reaches and encodes target location in an eye-centered reference frame.

This neuron exemplified the population of 74 neurons from three monkeys tested in this experiment. The data from all neurons are summarized by correlation analysis in Fig. 2A (*7*). Each point represents one neuron; a point's position along the horizontal axis represents the correlation between the cell's two tuning curves measured with targets at the same retinal location (conditions shown in Fig. 1, A and B). The position along the vertical axis represents the correlation between that neuron's tuning curves measured with targets at the same limb-centered location (conditions shown in Fig. 1, C and D). Eighty-four percent of the neurons lie below the line of equal correlation (*8*), showing a better correlation in an eye-centered reference frame than in a limb-centered reference frame. A second test was used in which the two tuning curves measured with the same initial hand position but with different eye positions were shifted into alignment in eye-centered coordinates (Fig. 2B). With this analysis, 81% of neurons had a correlation that was greater when the tuning curves were shifted into eye-centered alignment than when they were not shifted. Thus, the responses of most PRR neurons were better correlated for identical reach targets in eye coordinates than for identical reach targets in arm coordinates. For most neurons, spatial tuning was also more consistent in eye coordinates than in head- or body-centered coordinates; although target locations in the latter two reference frames were invariant across the four task conditions, neural responses varied with

Division of Biology and the Computation and Neural Systems Program, California Institute of Technology, Mail Code 216-76, Pasadena, CA 91125, USA.

*Present address: Howard Hughes Medical Institute and Department of Neurobiology, Stanford University School of Medicine, Fairchild Building, Room D209, Stanford, CA 94305, USA.
†Present address: Washington University School of Medicine, Department of Anatomy and Neurobiology, Box 8108, 660 South Euclid Avenue, St. Louis, MO 63110, USA.
‡To whom correspondence should be addressed. E-mail: andersen@vis.caltech.edu

the direction of gaze.

An eye-centered representation of a reach plan potentially may be disrupted if the eyes move before the reach can be executed, particularly if the reach is to a remembered location in the dark. Other brain areas involved in movement planning have been shown to update their spatial representations across saccadic eye movements and head movements (*9*). To test whether PRR can compensate for a saccade, we trained animals to make a saccade while planning a reach [the intervening saccide (IS) task] (*10*). The reach target was presented outside of or on the edge of the response field, and then, after the target was turned off, a saccade was instructed that brought the reach goal into the center of the response field. Figure 3C shows a neuron tested in this task. Before the monkey makes a saccade, the neuron's response is low, indicating the target is out of the response field (Fig. 3A). After the saccade, the neuron responds at a higher rate, similar to its response when the target actually appeared in the response field (Fig. 3B). A neuron was deemed to exhibit compensation for saccades if its response after the saccade was significantly greater (Mann-Whitney test, $P < 0.05$) than its response in the task where the target is presented out of the response field and no saccade is made (as in Fig. 3A) (*11*). All 34 PRR neurons that we tested showed compensation for saccades (Fig. 3D). Thus, PRR compensates for saccades to preserve correct encoding of reach targets in an eye-centered reference frame.

Psychophysical studies have provided evidence for a number of extrinsic coordinate frames for reach planning including eye-, head-, and shoulder-centered coordinates (*12*). Presumably the studies that find eye-centered effects are probing early planning stages in areas like PRR, which codes in eye coordinates.

There is suggestive evidence that PRR may work in conjunction with other areas to specify reach plans in eye coordinates. Lacquaniti *et al*. (*13*) found some area 5 neurons with reach activity that was more closely linked to the spatial location of the goal than to the direction of limb movement, although the paradigm they used did not allow them to determine the reference frame used by these cells. Although cells with response fields that are spatially invariant when the direction of gaze changes have been found in the area of the ventral intraparietal (VIP) [which has been suggested to play a role in head movements (*4*)], this is true of only about half the cells in VIP (*14*); the other cells in this area code in an eye-centered frame. Even in the premotor cortex, where limb-centered (*15*) and other nonretinal (*16*) response fields are found, about half the cells are still modulated by eye position (*17*), although it has yet to be established whether the response fields are in eye coordinates.

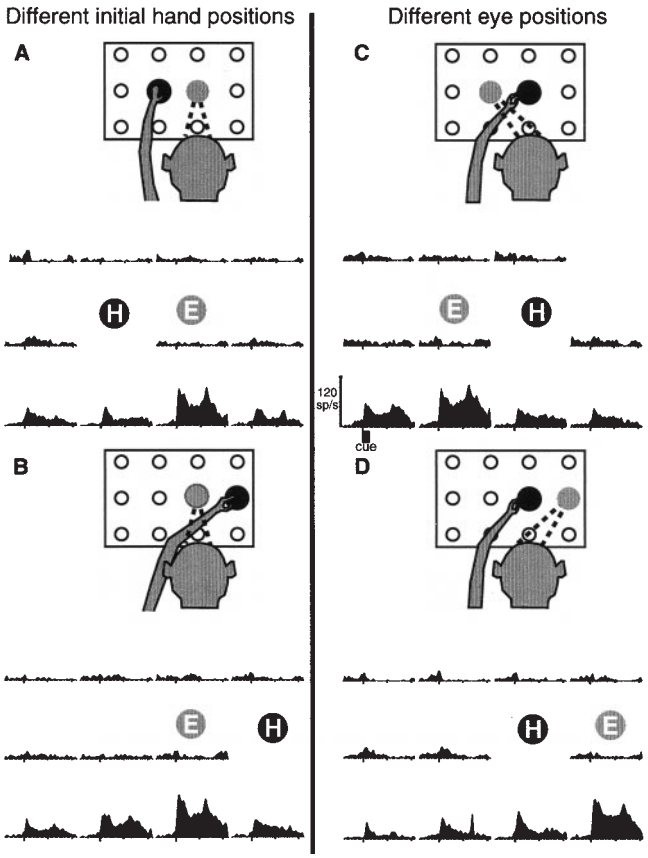

Fig. 1. Behavior of a PRR neuron in the coordinate frame task. (**A** to **D**) Responses of the cell for reaches made during one of the four task conditions. Icons depict behavioral conditions at the beginning of a trial: initial hand position and fixation are represented by solid black and gray circles, respectively; other target button locations are represented by open circles. Below each icon, spike density histograms (*28*) are plotted at positions corresponding to the target button locations on the board (11 locations in A, B, and D; 10 locations in C). Initial hand position and fixation position are indicated by H and E, respectively. Histograms are aligned at the time of cue onset, indicated by the long tic on the time axis. The cue was illuminated for 300 ms; its duration is marked in (C). Tic marks = 100 ms.

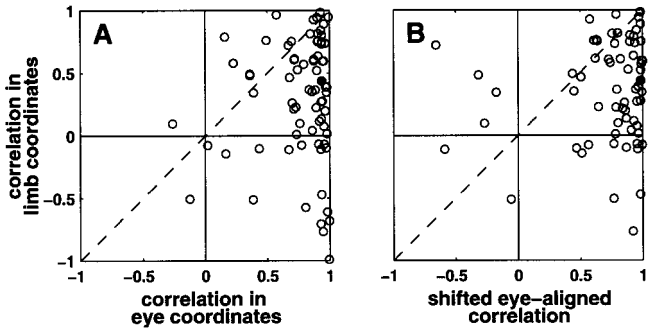

Fig. 2. Reference frame analysis for the population of reach neurons. (**A**) For each neuron (○), the correlation between the two tuning curves that have a common initial hand position (Fig. 1, C and D) is plotted on the vertical axis, and the correlation between the two tuning curves that have a common eye position (Fig. 1, A and B) is plotted on the horizontal axis. Seventy-four neurons are shown. Diagonal line represents equal correlation in limb-centered and eye-centered coordinates. Solid circle represents the neuron shown in Fig. 1. (**B**) Vertical axis is the same as in (A); horizontal axis is the correlation for the tuning curves collected with the same initial hand position but shifted into the same eye-centered alignment (data in Fig. 1C correlated with data in Fig. 1D shifted two buttons to the left).

Recent studies have emphasized that two largely nonoverlapping circuits, distributed through multiple brain regions, are responsible for eye movements (*18*) and reach movements (*19*). We propose that there is an initial stage in the multiarea reach circuit in which reaches are coded in eye-centered coordinates (Fig. 4). Response fields in a variety of areas in this presumed reach network, which includes PRR, area 5, and premotor cortex, are gain modulated by eye, head, and limb position signals. These gain fields can provide the mechanism necessary for the transformation (*20*) to later effector-centered reference frames such as limb-centered coordinates (Fig. 4). The few cells we found in PRR that were better correlated in a limb reference frame than in an eye reference frame, along with the cells with nonretinotopic and limb-centered fields in other reach areas, could reflect these later stages of movement processing. A prediction of this model, borne out by this study, is that for the transformation to operate correctly, neurons with eye-centered response fields must compensate for IS because eye position gains will necessarily change after the saccade.

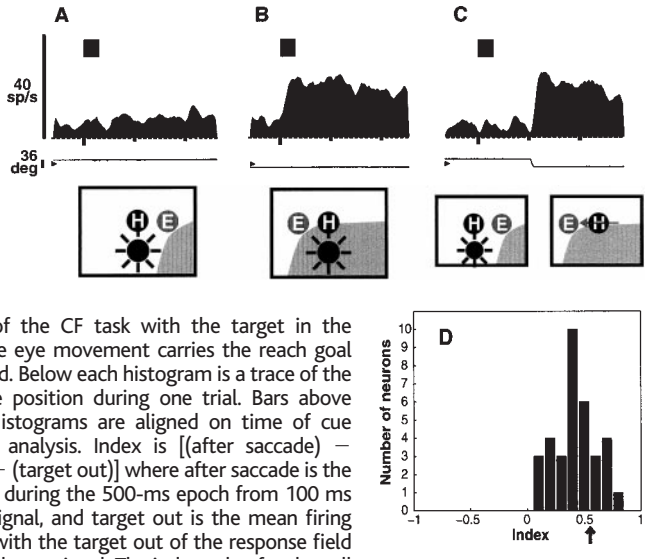

Fig. 3. (**A** to **C**) Behavior of one neuron tested in the intervening saccade experiment. The three spike density histograms show the response for reaches to the same target in the three tasks. The position of the response field is indicated by the gray region. (A) Condition of the CF task with gaze directed so that the target is out of the response field. (B) Condition of the CF task with the target in the response field. (C) IS task. The eye movement carries the reach goal into the neuron's response field. Below each histogram is a trace of the horizontal component of eye position during one trial. Bars above histograms, timing of cue. Histograms are aligned on time of cue presentation. (**D**) Population analysis. Index is [(after saccade) − (target out)]/[(after saccade) + (target out)] where after saccade is the mean firing rate in the IS task during the 500-ms epoch from 100 ms after the saccade to the go signal, and target out is the mean firing rate in the CF task condition with the target out of the response field (A) during the 500 ms before the go signal. The index value for the cell in (A) to (C) is indicated by the arrow.

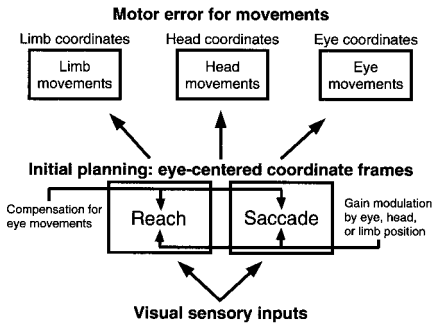

Fig. 4. Summary of pathways for sensory-motor control. Putative flow of information is from bottom to top.

In summary, our model proposes that initial plans to reach or make a saccade to a target are formed within distinct networks in eye-centered coordinates; these plans are updated if disrupted by IS; and finally, later stages of reach processing in head, body, and limb coordinates are achieved through gain modulations of the eye-centered representation.

There are several advantages to making reach plans in eye coordinates. First, natural scenes are cluttered with many potential reach goals as well as obstacles to reaching. If every object had to be converted to limb coordinates before formation of a planned reach, considerably more computation would be required than if the initial planning were performed in visual coordinates (*21*). Second, reach movements can be modified in flight by visual cues and cortical motor activity is correlated with these modifications (*22*). Because the hand is usually visible during reaching, it would be most parsimonious to make corrections to the reach plan in the same coordinates as on-line visual error signals. Third, the reach system is plastic, as has been demonstrated in adaptation experiments in which the visual feedback during reaching is perturbed with prisms (*23*). Clower *et al*. (*24*) have shown that the parietal cortex is uniquely involved in prismatic adaptation for reaches. Again the errors detected for adaptation are in eye coordinates, and this would be a most natural coordinate frame in which to recalibrate reach plans. Finally, planning reaches in eye coordinates may facilitate hand-eye coordination. Even in simple tasks, there is a complex orchestration of eye and hand movements, with the eyes and hands often moving independently to different locations (*25*). Nearby parietal area LIP is involved in planning eye movements and shares many similarities with PRR including eye-centered response fields, compensation for IS, and gain field modulation by eye position (Fig. 4). These two areas may use a similar encoding of space to enable fast and computationally inexpensive communication between them for simultaneous, coordinated movements of the eyes and arms. The above four considerations lead to the conclusion that the findings of this study, which at first glance appear quite surprising, are perhaps not so surprising after all.

References and Notes

1. M. Jeannerod, *The Neural and Behavioral Organization of Goal-Directed Movements* (Oxford Univ. Press, New York, 1988).
2. L. H. Snyder, A. P. Batista, R. A. Andersen, *Nature* **386**, 167 (1997).
3. A. Murata *et al.*, *J. Neurophysiol.* **75**, 2180 (1996).
4. C. L. Colby, *Neuron* **20**, 15 (1998); G. Rizzolatti, L. Riggio, B. Sheliga, in *Attention and Performance*, C. Umiltà and M. Moskovitch, Eds. (MIT Press, Cambridge, MA, 1994), vol. 15, pp. 231–265.
5. Recording sites were mapped onto the cortical surface in one animal (*2*); the other three animals are involved in other experiments. A nuclear yellow dye injection was made into a site where saccade-selective neurons were identified. This injection was visualized in the lateral bank of the intraparietal sulcus (area LIP). From the position of the dye injection and four pins marking the position of the recording chamber, PRR recording sites were localized to a region medial and posterior to LIP, presumably overlapping with areas V6A (*26*) and MIP (*19, 27*). Neurons were first examined in a delayed reach and saccade paradigm to determine their specificity for these two movement types (*2*). Eye movements were recorded with scleral search coils. Saccades and reaches were made to a vertically oriented 3 × 4 array of touch-sensitive buttons placed 24 cm in front of the animal. Each button was 3.7 cm in diameter and contained a red and a green light-emitting diode (LED) behind a translucent window 1.2 cm in diameter. A trial began with illumination of a red and a green LED at the button located straight ahead. The animal would look at and touch this button. A cue was presented (300 ms for monkeys D, G, and O; 150 ms for monkey C) at one of the eight locations surrounding the straight-ahead button, 18° or 26° from it. A red cue signaled an eventual saccadic eye movement [delayed saccade (DS) task], and a green cue signaled a reach [delayed reach (DR) task]. After a delay period (800 ms or longer), the central LEDs were extinguished as a "go" signal. The animal then made a saccade or reached to the remembered location of the target. Importantly, during saccade trials, the monkey could not move its hand, and, during reach trials, the animal had to maintain fixation at the location of the now-extinguished red LED. The contralateral limb was used in all experiments. The animal's room was dark; there was no vision of the hand during the reach. To test whether neurons were reach specific, delay period activity (from 100 ms after the cue was extinguished until the go signal) of the reach and saccade tasks was compared. If the greatest reach planning response was significantly larger than the greatest saccade planning response (Mann-Whitney test, $P < 0.05$), the neuron was considered reach-specific. Only reach specific neurons were analyzed further.
6. The coordinate frame (CF) task was a variant of the delayed reach task. Four conditions with different eye and initial hand positions were used. In two conditions, the red LED instructing visual fixation was at the button located straight ahead, and the green LED instructing the initial button press was 18° (36° for 11 neurons in monkey C) to the left or right. In these two conditions, target buttons were at identical locations in eye-centered coordinates but at different locations in arm-centered coordinates. In the other two conditions, the green LED was at the straight-ahead button, and the red LED was 18° to the left or right. In these conditions, target locations were identical in arm-centered coordinates but different in eye-centered coordinates. Reaches were typically made to between 8 and 11 buttons. The four conditions were otherwise identical to the delayed reach task. For each neuron, the four conditions were randomly interleaved for five repetitions of reaches to each target.
7. The average firing rate during the delay interval (from 100 ms after cue offset to the go signal) was used to compute the correlations. The formula used was

$$\text{correlation}(x, y) = \frac{\sum_{i=1}^{n}(x_i - \bar{x})(y_i - \bar{y})}{\sqrt{\sum_{i=1}^{n}(x_i - \bar{x})^2}\sqrt{\sum_{i=1}^{n}(y_i - \bar{y})^2}}$$

To compute the correlation in eye-centered coordinates, x_i is the average firing rate for a reach to a given target i from an initial hand position to the left, and y_i is a reach to the same target from an initial hand position to the right with the same fixation position, $\bar{x}$ is the average of the x_i, $\bar{y}$ is the average of y_i, and n is the number of targets that overlapped in the two configurations. To compute the correlation in hand-centered coordinates, x_i and y_i are the average firing rates for reaches to target i, with the eyes fixating to the left (x) or to the right (y) with the same initial hand position. For most cells, there were between 8 and 11 overlapping locations. If there were fewer than 3 overlapping locations, the cell was not included in the correlation analysis.
8. Ninety-one percent of neurons in monkey D (42 tested), 78% in monkey O (18 tested), and 71% in monkey C (14 tested) showed a greater correlation in eye-centered coordinates than in limb-centered coordinates.

9. L. E. Mays and D. L. Sparks, *J. Neurophysiol*. **43**, 207 (1980); J. W. Gnadt and R. A. Andersen, *Exp. Brain Res*. **70**, 216 (1988); J.-R. Duhamel, C. L. Colby, M. E. Goldberg, *Science* **255**, 90 (1992); M. F. Walker, E. J. Fitzgibbon, M. E. Goldberg, *J. Neurophysiol*. **73**, 1988 (1995); M. S. A. Graziano, X. T. Hu, C. G. Gross, *Science* **277**, 239 (1997).
10. The IS task was a modification of the CF task. Five hundred milliseconds into the delay period, the visual fixation point jumped. The monkey responded by making a saccade to the new location of the red LED. Another 600 ms of delay period ensued before both fixation LEDs were extinguished to trigger the reach. This task was interleaved with the two conditions of the CF task depicted in Fig. 1, C and D. In one of these conditions gaze was directed at the initial eye position for the IS trials. In the other condition, gaze was directed at the final eye position for the IS trials. The delay epochs for the two CF conditions were lengthened to 1100 ms to more closely match the overall delay period in the IS task. In all three tasks the initial hand position was at the center button, so the same reach was always performed. Typically, 10 repetitions of each task were performed.
11. Neurons that showed a significantly different response (Mann-Whitney test, $P < 0.05$) during the final 500 ms of the delay period for the two CF conditions were analyzed further. A cell was considered to update if its response during the 500 ms after the saccade and before the reach in the IS task was significantly greater (Mann-Whitney test, $P < 0.05$) than its response during the 500 ms before the reach for the CF condition with the target out of the response field. Fifteen neurons from monkey D, 16 from monkey O, and 3 from monkey G were studied.
12. D. Y. P. Henriques *et al.*, *J. Neurosci*. **18**, 1583 (1998); P. Vetter, S. J. Goodbody, D. M. Wolpert, *J. Neurophysiol*. **81**, 935 (1999); J. F. Soechting, S. I. H. Tillery, M. Flanders, *J. Cognit. Neurosci*. **2**, 32 (1990); J. McIntyre, F. Stratta, F. Lacquaniti, *J. Neurophysiol*. **78**, 1601 (1997).
13. F. Lacquaniti *et al.*, *Cereb. Cortex* **5**, 391 (1995).
14. J.-R. Duhamel *et al.*, *Nature* **389**, 845 (1997).
15. M. S. A. Graziano, G. S. Yap, C. G. Gross, *Science* **266**, 1054 (1994).
16. L. Fogassi *et al.*, *J. Neurophysiol*. **76**, 141 (1996).
17. H. Mushiake, Y. Tanatsugu, J. Tanji, *ibid*. **78**, 567 (1997); D. Boussaoud, C. Jouffrais, F. Bremmer, *ibid*. **80**, 1132 (1998).
18. C. Cavada and P. S. Goldman-Rakic, *J. Comp. Neurol*. **287**, 422 (1989); G. J. Blatt, R. A. Andersen, G. R. Stoner, *ibid*. **299**, 421 (1990).
19. P. B. Johnson *et al.*, *Cereb. Cortex* **6**, 1047 (1996).
20. D. Zipser and R. A. Andersen, *Nature* **331**, 679 (1988).
21. P. Sabes and M. I. Jordan, *J. Neurosci*. **17**, 7119 (1997).
22. A. P. Georgopoulos *et al.*, *Exp. Brain Res*. **49**, 327 (1983).
23. R. Held and A. V. Hein, *Percept. Motor Skills* **8**, 87 (1958).
24. D. M. Clower *et al.*, *Nature* **383**, 618 (1996).
25. D. H. Ballard *et al.*, *Philos. Trans. R. Soc. London Ser. B* **337**, 331 (1992).
26. C. Galletti *et al.*, *Eur. J. Neurosci*. **9**, 410 (1997).
27. C. L. Colby and J.-R. Duhamel, *Neuropsychologia* **29**, 517 (1991).
28. All spike density histograms were constructed by convolving spike trains with a triangular kernel, as described by D. W. Scott [*Ann. Statist*. **13**, 1024 (1985)].
29. Supported by the Sloan Center for Theoretical Neurobiology and the National Eye Institute. We thank Yale Cohen, Alexander Grunewald, and Philip Sabes for helpful discussions. We also thank Betty Gillikin and Viktor Shcherbatyuk for technical assistance, Janet Baer and Janna Wynne for veterinary care, and Cierina Reyes for administrative assistance.

29 June 1998; accepted 25 May 1999

BLyS: Member of the Tumor Necrosis Factor Family and B Lymphocyte Stimulator

Paul A. Moore, Ornella Belvedere, Amy Orr, Krystyna Pieri, David W. LaFleur, Ping Feng, Daniel Soppet, Meghan Charters, Reiner Gentz, David Parmelee, Yuling Li, Olga Galperina, Judith Giri, Viktor Roschke, Bernardetta Nardelli, Jeffrey Carrell, Svetlana Sosnovtseva, Wilbert Greenfield, Steven M. Ruben, Henrik S. Olsen, James Fikes, David M. Hilbert*

The tumor necrosis factor (TNF) superfamily of cytokines includes both soluble and membrane-bound proteins that regulate immune responses. A member of the human TNF family, BLyS (B lymphocyte stimulator), was identified that induced B cell proliferation and immunoglobulin secretion. BLyS expression on human monocytes could be up-regulated by interferon-γ. Soluble BLyS functioned as a potent B cell growth factor in costimulation assays. Administration of soluble recombinant BLyS to mice disrupted splenic B and T cell zones and resulted in elevated serum immunoglobulin concentrations. The B cell tropism of BLyS is consistent with its receptor expression on B-lineage cells. The biological profile of BLyS suggests it is involved in monocyte-driven B cell activation.

A 285–amino acid protein was identified in a human neutrophil-monocyte–derived cDNA library that shared identity within its predicted extracellular receptor-binding domain to APRIL (28.7%) (*1*), TNFα (16.2%) (*2*), and lymphotoxin-α (LT-α) (14.1%) (Fig. 1A) (*3*). This cytokine has been designated B lymphocyte stimulator (BLyS) on the basis of its biological activity. Analyses of the BLyS protein sequence have revealed a potential transmembrane spanning domain between amino acid residues 47 and 73 that is preceded by nonhydrophobic amino acids, suggesting that BLyS is a type II membrane-bound protein (*4*). Expression of this cDNA in mammalian cells [HEK 293 and Chinese hamster ovary (CHO)] and Sf9 insect cells identified a soluble form, 152 amino acids in length, with an NH_2-terminal sequence beginning with Ala^{134} (arrow in Fig. 1A). Reconstruction of the mass-to-charge ratio defined a mass for BLyS of 17,038 daltons, a value consistent with that predicted for this 152–amino acid protein with a single disulfide bond (17037.5 daltons). BLyS has been mapped to human chromosome 13q34 (*5*).

The expression profile of BLyS was assessed by Northern blot and flow cytometric analyses. BLyS is encoded by a single 2.6-kb mRNA expressed in peripheral blood mononuclear cells, spleen, lymph node, and bone marrow (Fig. 1B). Lower expression was detected in placenta, heart, lung, fetal liver, thymus, and pancreas. BLyS mRNA was also detected in HL-60 and K-562, but not in Raji, HeLa, or MOLT-4 cells. Surface expression was analyzed by flow cytometry with the BLyS-specific monoclonal antibody (mAb) 2E5. BLyS was not detected on T- or B-lineage cell lines, but was restricted to cells of myeloid origin, including K-562, HL-60, THP-1, and U-937 (*6*). Analyses of normal blood cell types showed expression on resting monocytes that was upregulated four times after exposure of cells to interferon-γ (IFN-γ) (100 U/ml) for 3 days (Fig. 1C). A concomitant increase in BLyS-specific mRNA was also detected by quantitative polymerase chain reaction using a TaqMan machine (Perkin-Elmer Applied Biosystems) (*6*). BLyS was not expressed on freshly isolated blood lymphocytes or on activated T cells [anti-CD3 mAb + interleukin-2 (IL-2)], B cells (SAC + IL-2), or NK cells (IL-2 + IL-12) (*6*).

Purified recombinant BLyS (rBLyS) was assessed for its ability to induce activation, proliferation, differentiation, or death in numerous cell-based assays involving B cells, T cells, monocytes, natural killer (NK) cells, hematopoietic progenitors, and a variety of cell types of endothelial and epithelial origin. A biological response to BLyS was observed only among B cells in a standard costimulatory proliferation assay in which purified tonsillar B cells were cultured in the presence of either formalin-fixed *Staphylococcus aureus*

Human Genome Sciences, 9410 Key West Avenue, Rockville, MD 20850, USA.

*To whom correspondence should be addressed. E-mail: david_hilbert@hgsi.com